ISSN 0145-8752, Moscow University Geology Bulletin, 2008, Vol. 63, No. 4, pp. 247–257. © Allerton Press, Inc., 2008.
Original Russian Text © P.Yu. Plechov, I.S. Fomin, O.E. Mel'nik, N.V. Gorokhova, 2008, published in Vestnik Moskovskogo Universiteta. Geologiya, 2008, No. 4, pp. 35–44.

Evolution of Melt Composition during Intrusion of Basalts into a Silicic Magma Chamber

P. Yu. Plechov, I. S. Fomin, O. E. Mel'nik, and N. V. Gorokhova

Received November 13, 2007

Abstract—The article describes heat exchange between basaltic and rhyolite melts accompanied by fractional crystallization of phases in a basaltic melt. A numerical model has been developed for the homogenization mechanism of magma composition during intrusion of basaltic magma batches into felsic magma chambers. The results of numerical modeling demonstrate that the time needed for cooling the basalts and their fractionation to rhyolite melts is much shorter than the time required for chemical interaction based on diffusive mechanisms.

DOI: 10.3103/S0145875208040054

INTRODUCTION

The idea of mixing of magmas with different compositions was developed based on geological and petrological studies of andesite-dacite island-arc volcanic centers [Eichelberger, 1978]. The main mechanism of such mixing is the transport of batches of the basic and intermediate (basaltic and andesitic) magma into a crustal magma chamber, which usually contains more silicic (dacitic, rhyolite-dacitic, and rhyolite) magma. Such magma systems are commonly found in the islands arc tectonic settings, which are characterized by long-lived chambers of silicic magma.

Mixing of magmas is manifested in silicic-to-basic sequences of eruptions; synchronous eruption of basalts and hybrid rocks; resorption of phenocrysts; complex zoning of minerals, non-equilibrium associations of phenocrysts, appearance of reaction rims of minerals around other minerals, abundance of mafic enclaves, and presence of contrast groups of melt inclusions [Popov, 1983; Bacon, 1986; Murphy at al., 2000; Naumov et al., 1997; Eichelberger et al., 2006; Plechov et al., 2000, 2008; Trusov and Plechov, 2005]. Some authors [Annen et al., 2006] have demonstrated that large magmatic intrusive bodies consist of many separate batches of magma that were intruded sequentially and finally merged into one magmatic body. Thus, mixing and equilibration of a new magma batch should occur repeatedly.

NON-EQUILIBRIUM MINERAL ASSOCIATIONS

Crystals that crystallized before mixing in one of the magmas are conserved during a certain period of magma mixing. For example, if a basaltic magma containing olivine intrudes into a rhyolite magma containing quartz, and eruption occurs earlier than the quartz and olivine are dissolved or re-equilibrated with the newly formed melt, the new rock will contain a non-equilibrium set of minerals. During mixing, at least one (or two, if the composition of the matrix melt and conditions change significantly) of the previously existing mineral associations starts a reactive interaction with the matrix melt, which can be reflected in the reactions of the minerals, that crystallized earlier, with the melt. Association of high-calcium plagioclase, Al-hornblende, high-Mg olivine and chromium spinel with sodic plagioclase, low-Al amphibole, quartz, and rhyolite matrix is an example of non-equilibrium associations of phenocrysts [Feeley et al., 1996; Clynne, 1999; Costa and Singer, 2002; Trusov and Plechov, 2005].

If we assume that a near-surface chamber in a long-lived volcanic center is filled with silicic magma, whereas the inflowing batches are presented by more basic magma, then not only a temperature increase will occur in a given region of the magma chamber due to mixing, but also the melt composition will be displaced to a more basic range. If new physicochemical conditions are maintained within the stability fields of previously crystallized minerals, this should lead to the formation of impregnation zones within the chamber with more magnesian zones in mafic minerals and higher-calcic zones in plagioclases. As complex zoning patterns are often observed in erupted minerals, this implies that the rate of diffusive re-equilibration of crystals is low compared to the periodicity of intrusions of magma batches and eruptions.

Lack of equilibrium between an impregnated material and the matrix melt is demonstrated by the formation of reaction rims around minerals which are unstable under the new conditions. Clinopyroxene rims around orthopyroxene, and quartz with clinopyroxene rims, are the most common [Eichelberger, 1978; Murphy et al., 2000], pargasite rims around biotite [Nakada et al., 1997]. Olivine crystals with amphibole or pyroxene rims were also described [Dirksen et al., 2006]. It has been shown that reaction rims around phenocrysts

are common in island arc dacite and andesite, and they can be formed due to heating of rhyolite magma in the chamber by basaltic injections [Plechov et al., 2008].

Melt inclusions in minerals, which crystallized in both magmas before mixing, can conserve unmixed melts. The composition of a rock matrix can reflect the melt composition, which formed already as a result of mixing. Naumov et al., [1997] demonstrated statistically that melt inclusions of basalt, andesite-basalt, dacite-rhyolite, and rhyolite compositions dominate in island-arc systems, whereas melt inclusions of andesite composition are practically absent there, which implies hybrid genesis of in island-arc andesites due to mixing of basaltic and rhyolite magmas.

Melanocratic enclaves. Eruption products of many andesite and dacite volcanoes in island arcs contain numerous melanocratic enclaves. Some examples include Unzen (Japan) [Nakada, 1997], Pinatubo (Philippines) [Pallister et al, 1996], Soufriere Hills (Montserrat) [Murphy et al., 2000] as well as Kamchatka volcanoes Bezymyannyi [Gorshkov and Bogoyavlenskaya, 1965], Shiveluch [Dirksen, et al., 2006], Kizimen [Trusov and Plechov, 2005], and Dikii Greben [Bindeman, 1993].

POSSIBLE MECHANISMS OF INJECTION AND FRAGMENTATION OF BASALTIC MAGMA

It is likely that intrusion mechanisms of basaltic magma into silicic chambers can be different for different volcanoes. For example, Annen and Sparks [2002] suggested periodic intrusions of basaltic dikes into a partly

melted chamber as one of the main mechanisms. In this case, the intruded magma can later disintegrate into

fragments due to convection. Another option is relatively slow seeping of basaltic magma through cracks in the walls of the chamber and its entrainment in the convection occurring in the chamber. Finally, formation of a two-layer chamber is possible as a result of the density difference between basaltic and rhyolite melts. Heat exchange between magmas occurs at the boundary between layers. Crystallization of basaltic magma can lead to its oversaturation in volatile components, formation of bubbles, and uplift of basaltic magma droplets. Formation of compact volumes of basaltic magma, which later react with the surrounding rhyolite melt, cool and crystallize, is possible by any of the above mechanisms. It is likely that these compact segregations exist in the magma chamber in the form of individual globules of different sizes, whereas in the eruption products they are observed as melanocratic enclaves. The sizes of melanocratic enclaves in island-arc volcanics vary from of a millimeter to a few meters scale. Bindeman [1993] gives a size distribution of melanocratic enclaves for the Dikii Greben Volcano (Kamchatka). The sizes of enclaves are distributed closely to a lognormal distribution and vary from 1 to 20 cm with the maxima of distribution in the range of 2–5 cm. Variations in the sizes of basaltic magma fragments can be derived from such observations, as described below.

FORMULATION OF THE PROBLEM AND MATHEMATICAL MODEL

Description of Possible Mechanism of Injection

We suggest the following mechanism of the interaction between injections of basic magma with the material in near-surface chambers of silicic composition. Injections of basic magma ascend and intrude into the near-surface chambers as dikes. Once inside the viscous medium of the silicic melt, they continue their ascent and deform due to the resistance of the viscous medium and existing convection currents within it. The velocity of convection currents in a viscous medium is not high, and we assume the distance of material transport due to this mechanism to be in the range of several meters. During this process, fragmentation of the intruded magma occurs, and globules of different sizes originate and spread over the volume of the magma chamber. During the movement of globules in the viscous medium, mechanical trapping of external phenocrysts from the surrounding magma is possible. Basaltic magma begins crystallizing due to a sharp temperature contrast. This crystallization is predominantly fractional because the crystallization time is short as compared to the time needed for attainment of equilibrium via diffusive exchange within crystallizing phenocrysts. The surrounding magma heats up due to heat exchange with the intruded basalt and the latent heat released during crystallization of basaltic globules.

Thermal re-equilibration of basaltic globules with the surrounding melt causes mass crystallization of minerals from the basaltic melt. The quantity and composition of the residual melt, which forms during this process within the globules, will be mainly a function of temperature, to which magma attains as the result of thermal equilibration. Since the temperature in the globules and around them remains the same after reaching equilibrium, we can expect similar compositions of melts in the globules and in the surrounding magma. Time during which the residual melt can remain within the system is limited by the general cooling of the magmatic system. Partly recrystallized globules located in the magma chamber during a long period would gradually decompose into individual crystals and glomeroporphyric aggregates. During this process, the residual melt from the globules will be able to mix with the matrix melts of the surrounding magma. Mafic minerals (for example, olivine) formed during crystallization of basalt magma react with the residual melt and completely disintegrate over 4–12 years depending on the size of the grains [Coombs et al., 2004; Dirksen et al., 2006]. Pyroxene can diffusively re-equilibrate with the magma during approximately the same time interval.

The diffusion rate of CaAl–NaSi in plagioclase is extremely slow; therefore, plagioclase often maintains complex zoning during the lifespan of a magma chamber.

It follows from the above that direct mixing of basaltic and rhyolite melts is not common. The process of interaction of rhyolite with subordinate amounts of basalt likely occurs in several stages. First, basaltic magma crystallizes, forming crystals and the residual melt. During the second stage, the residual melt mixes with the matrix melt of the surrounding magma, and the crystals partially or completely re-equilibrate with the same matrix melt. During new injections of basalts and renewed heating of the magma chamber, these crystals can dissolve partially or completely, modifying the composition of the matrix melt.

In this article we present the results of numerical modeling of the evolution of basaltic globules in a silicic magma chamber. The modeling takes into account crystallization of the basaltic melt and heat exchange with the surrounding magma.

Description of the system and the initial and boundary conditions. For the description of heat exchange and crystallization of basaltic batches, we assume that a batch of basaltic magma separates into spherical drops with a radius R during its intrusion into a rhyolite melt. These drops are located at equal distances from each other. Each drop is surrounded with a spherical shell of the rhyolite melt, which absorbs heat from it, together forming a cell. We assume that N cells are located in a volume unit (for example, in 1 m^3). Then, the external radius of each cell S is determined by $4\pi R^3 N/3 = \alpha$ assuming that the cells completely cover the total volume of magma. Such a cell model for presenting a multi-phase system was successfully used for modeling the dynamics of bubble growth in magma [Navon et al., 1998]. We assume that distribution of parameters in each cell is characterized by central symmetry, i.e. it depends only on the radius of the radial coordinate r.

We assume that the fragmentation time of a basalt melt is sufficiently shorter compared with the time of its cooling so that we can neglect the cooling of the basaltic melt during fragmentation. Modeling of cooling of the individual drops, which would allow for a quantitative estimation of the required rate of basaltic melt fragmentation, will be presented elsewhere. On the basis of these assumptions, the initial temperature distribution $T(r, t = 0)$ in the cell is given by formula 1

$$T(r, t = 0) = \begin{cases} T_\beta, & 0 < r < R \\ T_r, & L < r < S, \end{cases} \quad (1)$$

where the indices β and r denote temperatures of basalt and rhyolite magmas.

Heat Transport

In order to describe the temperature within a cell, we shall write the equation of heat flow in a reference volume V formed by the intersection of a spatial angle (opening angles $d\varphi$, $d\psi$) with spheres of radii r_1 and r_2 ($r_2 - r_1 = dr$):

$$\frac{d}{dt}\int_V U dV = \int_V Q dV + \int_\Sigma F d\Sigma, \quad (2)$$

where U is the internal energy in a unit volume of magma, Q is the power of heat sources (in this

case, they are related to the release of the latent heat of crystallizations), F are the heat fluxes through the volume boundary V, and t is time. Due to the spherical symmetry of the problem, we can integrate the equation with respect to angles φ and ψ from zero to 2π, and rewrite equation (2) as

$$\frac{4}{3}\pi(r_2^3 - r_1^3)\frac{\partial}{\partial t}\langle U\rangle = \frac{4}{3}\pi(r_2^3 - r_1^2)\langle Q\rangle + 4\pi(r_2^2 F_2 - r_1^2 F_1), \quad (3)$$

where the values in brackets are the volume average internal energy and power of heat sources. Fick's law is applicable to heat fluxes through the corresponding boundaries:

$$F_i = -k\,\mathrm{grad}(T)_{r = r_i} = -k\left(\frac{\partial T}{\partial r}\right)_{r = r_i}; \quad i = 1, 2, \quad (4)$$

where k is the coefficient of magma heat conductivity, which depends on its chemical composition, but can be considered constant as first approximation. We describe the internal energy as a function of magma density, its heat capacity, and temperature. Owing to the fact that magma consists of a melt and different crystals, its density and heat capacity are combined from the sum of densities and heat capacities of individual components. Let us introduce mass fractions of crystals in magma x_j. Then, the mass fraction of the melt x_m is written as:

$$x_m = 1 - \sum_{j=1}^{n} x_j, \quad (5)$$

where n is the number of crystal types in the melt. We can represent the internal energy as

$$U = \left(\rho_m x_m C_m + \sum_{j=1}^{n} \rho_j x_j C_j\right) T, \quad (6)$$

where ρ_j are the densities of the melt and crystals and C_j are specific heat capacities. If we ignore the differences in heat capacities and densities between the melt and crystals, we can use a simpler equation $U = \rho C T$

instead of (6), where ρ and C are the mean values of density and heat capacity. Release of the latent heat of crystallization is an additional heat sources that can be described as:

$$Q = \sum_{j=1}^{n} L_j \rho_j \frac{\partial x_j}{\partial t} = \left(\sum_{j=1}^{n} L_j \rho_j \frac{\partial x_j}{\partial T} \right) \frac{\partial T}{\partial t} + \left(\sum_{j=1}^{n} L_j \rho_j \frac{\partial x_j}{\partial p} \right) \frac{\partial P}{\partial t}, \quad (7)$$

where L_j is the latent heat of crystallization of the corresponding component, and P is pressure.

Equation (7) stands if we ignore crystallization kinetics and assume that mass fractions of individual crystals are determined by temperature and pressure only. The boundary conditions for equation (3) are: temperature at $r = 0$ cannot increase and heat flux is 0 at $r = S$. Equation (3), together with equations (4–7), is solved numerically at each time step, together with the equations describing crystallization of the melt. The crystallization model is described in the next section.

Modeling of Crystallization

Thermodynamic mineral-melt models for olivine, clinopyroxene, orthopyroxene, plagioclase, and magnetite were applied for modeling the evolution of a basaltic melt and release of latent heat at each point of the profile. These models estimate the composition of the mineral and its crystallization temperature for a given composition of the melt [Ariskin and Barmina, 2000]. The mineral-melt models were solved for mineral stoichiometry:

$$\Delta C = K - \exp(f(T, P, F_{O_2}, C_i^m)), \quad (8)$$

where ΔC is the deviation from stoichiometry, K is the stoichiometric coefficient, F_{O_2} is the fugacity of oxygen, C_i^m are concentrations of main components in the melt. Equation (8) is solved for each mineral with respect to temperature using a numerical method of "dividing the segment into halves" for the condition of convergence of ΔC to zero. The crystallized mineral is determined following the van Kirk law [Ariskin and Barmina, 2000] as the mineral with the maximum calculated temperature. Crystallization of a given mineral is described by mass-balance equations for each melt component (C_i^m, C_i^s are concentrations of major-element oxides in the melt and in the solid phase, respectively, s is the mass increment of crystallization):

$$C_i^m = \frac{C_i^m - sC_i^s}{-s}. \quad (9)$$

The crystallization increment was assumed to be equal to 10^{-6} of the existing melt amount. On each step, crystallization at each point within the cell continuous until temperature corresponds to that obtained from the solution of the heat conductivity equation for the given point of the profile through the cell. The latent heat of crystallization is calculated from:

$$L = \sum_i \sum_k \Delta H_{i,k} \Delta x_{k,i}, \quad (10)$$

where L is heat, ΔH_i is the enthalpy of crystallization of component i, and Δx_k is the amount of the component crystallized at step j.

NUMERICAL METHOD

Let us introduce a mesh with step $h_k = r_{k+1} - r_k$ over interval $r \in (0, S$. Then equations (3) and (5) can be rewritten as

$$\frac{U_k - \tilde{U}_k}{\Delta t} = Q_k + \omega(r_{k+1}^2 F_{k+1} - r_k^2 F_k); \quad \omega = \frac{3}{(r_{k+1}^3 - r_k^3)}; \quad F_k = -k\frac{(T_k - T_{k-1})}{h_{k-1}}. \quad (11)$$

Equation (11) is a non-linear difference equation with respect to temperature, because the term responsible for the power of heat sources depends in a complex nonlinear manner on temperature (see equation (7)). After linearization, equation (11) is reduced to a three-point equation relating temperatures at points $k - 1$, k, and $k + 1$. It is solved using the sweep method together with the differential analogs of the boundary conditions. In the case where the mass fractions of minerals depend only on temperature, it is possible to redefine the internal energy of the cell as:

$$U = \left(\rho C - \sum_{j=1}^{n} L_j \rho_j \frac{dx_j}{dT} \right) T. \quad (12)$$

In this case, the heat sources component in equation (11) can be neglected.

A flow chart of the algorithm for calculation of magma temperature is shown in Fig. 1. The temperatures of basaltic and rhyolite magmas and their compositions are specified at the initial time step. After this, at each time step, we calculate magma crystallization and released heat and correct the temperature based on solution of equation (11). The calculations are terminated when the difference of temperature values in the center and at the outer boundary of the cell become less than a predefined value.

APPLICATION OF THE MODEL TO NATURE

Below we will discuss as an example the magmatic system of the Kizimen Volcano (Kamchatka). All the indicators for the supply of basaltic magma to a rhyolite chamber described above are pertinent to this volcano [Trusov and Plechov, 2005; Churikova et al., 2007]. Churikova et al., 2007 emphasized the abundance of large melanocratic enclaves (up to 35 volume percent) in lavas of Kizimen Volcano with a size up to 30–35 cm. The melanocratic enclaves consist of basalts and andesitobasalts which contain phenocrysts of olivine, plagioclase, and clinopyroxene. Olivine contains inclusions of chrome spinel. Plagioclase phenocrysts commonly contain essentially unzoned cores (sometimes with a sieved texture) of high-Ca composition ($An_{91–97}$) [Trusov and Plechov, 2005]. The outer zone of plagioclase phenocrysts, up to 40–50 μm wide, is characterized by very sharp normal zoning down to An_{49}, which closely matches the compositions of plagioclase microlites in these enclaves ($An_{48–53}$). Such rims around unzoned cores of plagioclase reflect near-fractional crystallization that occurred after fragmentation of the basaltic melt into individual drops. We believe that the resorbed crystals of amphibole, orthopyroxene, and complexly zoned sodic plagioclase within melanocratic enclaves represent minerals from the surrounding magma that were mechanical trapped during intrusion of the basaltic magma into the chamber and its consequent fragmentation.

Compositions and P–T–fO_2 conditions of the rhyolite and basaltic magmas involved in the mixing process were reconstructed on the basis of investigation of phenocryst assemblage and melt inclusions in phenocrysts. The composition of melt in the magma chamber was estimated based on the compositions of glassy melt inclusions in orthopyroxene phenocrysts (28 compositions, wt %): SiO_2 74.1–80.2; TiO_2 0.06–0.9; Al_2O_3 10.33–14.24; FeO 0.91–2.54; MnO 0.1–0.5; MgO 0.02–0.22; CaO 0.2–2.6; Na_2O 2.2–4.7; K_2O 2.0–3.7. The compositions of glasses of the matrix of the specimen in which inclusions were studied are identical to the inclusions. This allows us to ignore the effect of mixing processes on the composition of the silicic magma. Thus, the long-lived magmatic chamber under the Kizimen Volcano is filled with rhyolite melt containing an assemblage of plagioclase-amphibole-orthopyroxene-titanomagnetite-ilmenite phenocrysts. This magma chamber is at a depth of 4-6 km and temperature of 750–825°C [Trusov and Plechov, 2005] and is the likely source of material for explosive eruptions and extrusive domes. The average composition of melt inclusions in olivine from melanocratic enclaves is (mean values over 12 inclusions, wt %): SiO_2 46.34; TiO_2 1.5; Al_2O_3 19.96; Fe_2O_3 1.62; FeO 8.72; MnO 0.16; MgO 5.27; CaO 11.75; Na_2O 3.47; K_2O 0.83. The temperature of this melt was estimated at 1110–1120°C and oxygen fugacity at the level of the NNO buffer [Trusov and Plechov, 2005].

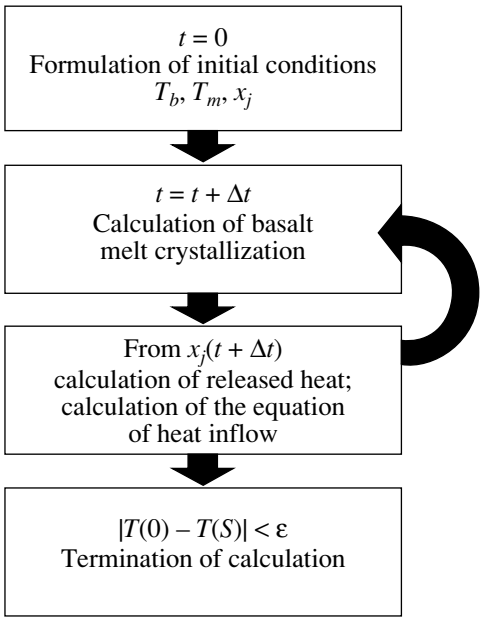

Fig. 1. Flowchart of algorithm for numerical modeling of crystallization within globule and accounting for heat exchange with the surrounding magma. Notations: T_b and T_m are the temperatures of basalts and rhyolites, respectively; x_j is basalt composition, t is time.

Modeling parameters. We assumed that globules have spherical shapes and that their radii vary from 0.5 to 32 cm. Calculations were performed for basalt contents of the magma of 10, 15, 20, 25, 30, and 35 vol %, intruded into a rhyolite magma chamber. Bindeman [1993] demonstrated that the overall proportion of basalt is such systems is likely to be within 4–10 vol %, however it can be much higher at fragmentation fronts. The P–T–fO_2 parameters for the magma chamber and intruded basalts were taken from [Trusov, Plechov, 2005]. Basalt temperature during intrusion was assumed to be 1390 K (1117°C); the temperature of the magma chamber prior to basalt intrusion was assumed to be 1023 K (750°C), and the pressure in the system was assumed to be 0.14 GPa. A constant Fe^{2+}/Fe^{3+} ratio in the melt (4.8) was assumed in the calculations. Oxygen fugacity was assumed to correspond to the NNO buffer. We assumed pure fractional crystallization of the basaltic melt, i.e., the crystallized phases were not re-equilibrated with the residual melt. The latent heat of crystallization was estimated from the values of crystallization enthalpy $\Delta H_{olivine} = 63.35$; $\Delta H_{plagioclase} = 101.42$; $\Delta H_{clinopyroxen} = 147.78$; $\Delta H_{orthopyroxene} = 70.46$; $\Delta H_{magnetite} = 138.16$ kJ/mol [Wood, 1992]. Heat conductivity, heat capacity, and density of basalt and rhyolite were assumed constant and equal to 1 W/(m K), 1200 J/(kg K), and 2500 kg/m^3, respectively.

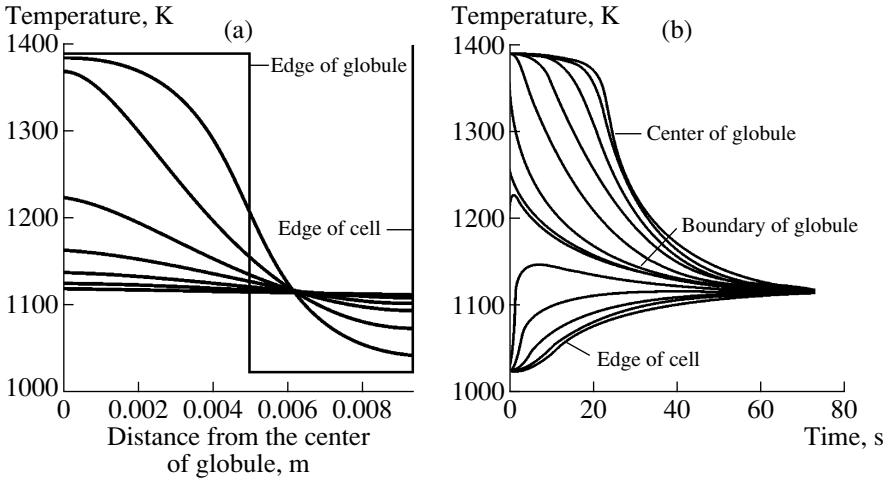

Fig. 2. Distribution of temperature over the profile of calculation cell at for 15% basalt melt in rhyolite within globule of 1-cm diameter. Time step is 10 s (a) and time dependence of temperature in different parts of the system. Calculation for a 15-percent basalt melt is shown in the system and globule diameter is 1 cm (b).

Selection of the Starting Compositions

As was shown above, melanocratic inclusions are contaminated with plagioclase, amphibole, and orthopyroxene phenocrysts from the host dacites. It is possible that the melt from the magma source also penetrated in small amounts into the globules. On the other hand, a portion of the residual melt could have mechanically escaped the globules after establishing thermal equilibrium. Thus, the composition of melanocratic enclaves depends on many local factors and is therefore variable. We cannot consider the composition of melanocratic enclaves representative of the composition of the intruding basalts.

The compositions of melt inclusions in minerals from globules may reflect the composition of the basaltic at the moment of intrusion, however, they cannot reflect the composition of the basaltic magma as a whole, as it is a mixture of the melt and phenocrysts.

For the purpose of our modeling we used the composition of lavas from the Tamara Cone as the initial composition of the basaltic magma. This cone is located 12 km to the northwest of the volcano summit. It is the only remaining basaltic eruption center from those that existed prior to formation of the Kizimen Volcano [Melekestsev et al., 1992]. The lavas from the Tamara Cone do not contain evidence for mixing such as non-equilibrium phenocryst assemblages [Melekestsev et al., 1992]. We thus assume that the composition of these lavas can be used as an estimate for the batches of basaltic magma transported to the near-surface magma chamber during the evolution of the magmatic system of the Kizimen Volcano. It is worth noting that this composition has a calculated liquidus temperature of approximately 1190°C. At the temperature of intrusion (1117°C, see above), this composition will be crystallized to approximately 40 wt %. Modeling of crystallization of this composition shows that at the moment of intrusion phenocrysts of plagioclase (approximately 30 wt %) and olivine (approximately 8 wt %) were present in the magma. This corresponds well to the petrographic observations made for the Kizimen enclaves. The choice of the initial composition for the silicic magma is not essential as crystallization and melting of minerals within the rhyolite magma are not considered.

CALCULATION RESULTS

Temperature Evolution for the Basalt–Rhyolite System

The process of reaching temperature equilibrium due to heat exchange leads to cooling of basalts, accompanied by crystallization of minerals, and to heating of the rhyolite. This process is most important at the interface between the two magmas. Figure 2 shows the distribution of temperature as a function of time, calculated from equations (3–7) reduced to a nonlinear equation of heat conductivity where heat capacity is a function of temperature. At constant pressure, crystallization occurs due to cooling only; thus, release of the latent heat of crystallization leads to an increase in the effective heat content of the basaltic magma. Thus the rate of cooling of the basaltic magma decreases. However this process cannot lead to the increase of temperature of the basaltic magma, as crystallization and corresponding release of the latent heat would stop immediately. The temperature of the basaltic magma decreases monotonously with time and increasing distance from the center of the drop (Fig. 2b). The rhyolite magma near the interface initially becomes hotter than the temperature of the final thermal equilibrium and, therefore, its temperature then also monotonously decreases with time reaching the equilibrium value. Temperature of the rhyolite magma

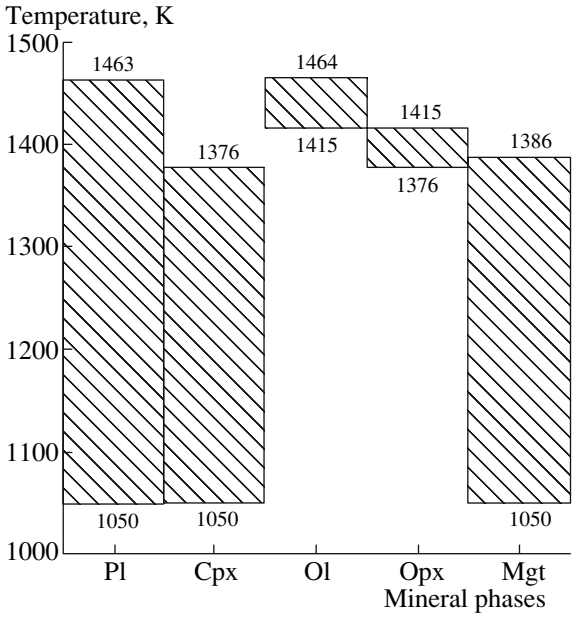

Fig. 3. Sequence of crystallization for the starting composition. See the Text for description.

far from the interface shows a different behavior increasing continuously until it reaches the temperature of the final thermal equilibrium.

Sequence of mineral crystallization. The model basaltic melt at the initial *PT*-parameters has a liquidus assemblage of olivine ($Fo_{81.1}$) and plagioclase ($An_{93.0}$) at 1190°C (1463 K), which agrees well with the petrography of lavas from the Tamara Cone [Melekestsev et al., 1992], the petrography of melanocratic enclaves, and the described relict assemblages in dacites of the Kizimen Volcano [Trusov and Plechov, 2005]. The lower temperatures of the basaltic melt recorded by the melt inclusions in olivine likely reflect intermediate stages of cooling of the fragments of the basaltic melt within the dacitic host.

At a temperature of 1142°C (1415 K), olivine is replaced by orthopyroxene (Fig. 3). In the melanocratic enclaves in the volcanics of the Kizimen Volcano, olivine is often rimmed by orthopyroxene, confirming modeling results. At a temperature of 1113°C (1386 K), magnetite starts to crystallize together with plagioclase and orthopyroxene. Magnetite was found in the studied samples along with orthopyroxene in the rims around olivine and also as separate crystals. At a temperature of 1103°C (1376 K), orthopyroxene is replaced by clinopyroxene, which was observed in melanocratic enclaves in the matrix between large crystals, which also contains plagioclase and oxide minerals. Needle- and elongated prismatic-shaped clinopyroxene in the melanocratic enclaves (for example, in Sp. TR-01/12) also provide evidence that it crystallized at the latest stages from an under-cooled melt.

The final proportion of the crystallized phases in the basaltic globules depends on the final temperature of the established thermal equilibrium. At the maximum temperature of thermal equilibrium (960°C; 1233 K), reached during injection of 35% of the basaltic magma within 58 hours, the proportion of phases in the globules is (in mol %): 49.5% plagioclase, 8.3% olivine, 11.4% clinopyroxene, 7.6% orthopyroxene, 6.9% magnetite, and 16.3% rhyolite melt (SiO_2 75.06 wt %). At the minimum temperature of thermal equilibrium (813°C; 1086 K), reached during injection of 10% of the basaltic melt within 101 hours, the proportion of phases in the globules is (in mol %): 51.4% plagioclase, 8.3% olivine, 12.1% clinopyroxene, 7.6% orthopyroxene, 7.1% magnetite, and 13.5% rhyolite melt (SiO_2 76.97 wt %).

Evolution of the melt chemical composition. The model basaltic melt evolves strongly during crystalliza-

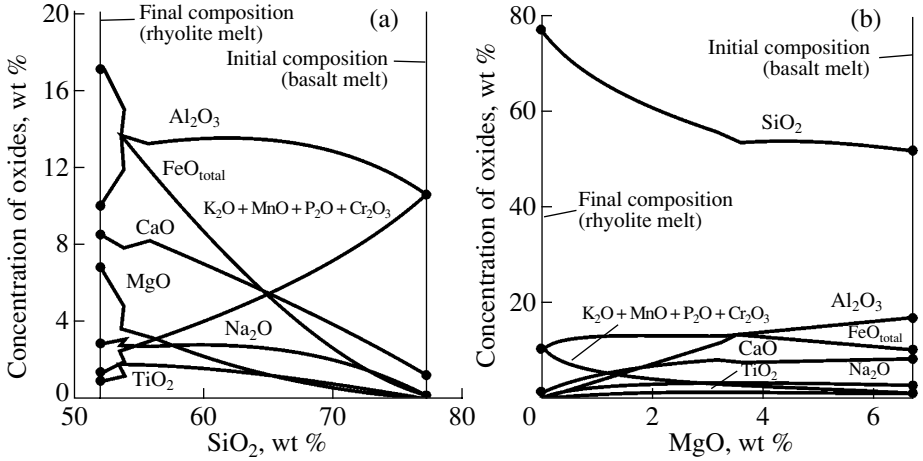

Fig. 4. Diagrams demonstrating the chemical evolution of the residual melt within globule for magmatic system of the Kizimen Volcano in coordinates (a) SiO_2-oxides; (b) MgO-oxides.

Relationship between the radius of basalt globules, ratio of magma volumes, and time (c) needed for reaching thermal equilibrium. The temperature with accounting for latent heat is T_{cr}; the temperature without accounting for latent heat is T_{eq}

Radius of globules, m	Volume proportion of basalts, *a*					
	0.1	0.15	0.2	0.25	0.3	0.35
0.005	90	73	65	57	54	51
0.01	358	294	257	233	214	206
0.02	1434	1171	1022	924	855	814
0.04	5746	4705	4100	3697	3432	3262
0.08	23013	18852	16431	14829	13755	13128
0.16	91791	75194	65499	59059	54705	52129
0.32	365760	299240	260500	234540	216760	205940
T_{cr}, K	1089	1118	1149	1179	1208	1233
T_{eq}, K	1065	1083	1103	1121	1140	1156

tion of minerals within globules. Cotectic crystallization of olivine and high-calcic plagioclase leads to a change in the composition of the melt to the andesitic range (up to 53.77 wt % SiO_2) and sharp decrease in alumina (up to 13.73 wt %) and magnesium oxide (up to 3.6 wt %) accompanied by an increase in iron (up to 13.65 wt % of FeO total) (Figs. 4a and 4b). During further crystallization of plagioclase, orthopyroxene, and magnetite, the content of iron in the melt decreases, while the content of silica increases sharply. This increase in the silica content is due to the crystallization of magnetite shifting the silica content to above 54–55 wt %, the level at which crystallization of any rock-forming mineral in this system (excluding quartz) leads to increasing silica content in the residual melt. As a result of fractionation, the residual melt contains: 75–77% SiO_2; 0.01–0.93% TiO_2; 10.72–11.53% Al_2O_3, 0.18–0.67% FeO total; 0.03–0.15% MgO; 1.35–2.16% CaO; 0.27–0.87% Na_2O, and 6.82–7.55% K_2O. The final degree of fractionation of the basaltic magma at different proportions of basalt to rhyolite remains essentially the same at thermal equilibrium, because the degree of fractionation at a temperature below 950°C changes only slightly with temperature. These compositions agree well with the compositions of silicic melts analyzed in melt inclusions in orthopyroxene from the Kizimen Volcano. A strong difference between the analysed and modeled compositions was recorded for components that are not included in the mineral–melt equilibrium models such as K_2O and MnO.

Thus, within the range of parameters used for modeling, basalt fractionation results in 13.4–14.9% of the initially intruded volume being a residual melt of rhyolite composition, which is in thermal equilibrium with the host magma within the chamber.

Temperature of final thermal equilibrium as a function of the proportion of the basaltic melt. As was shown above, as the result of heat exchange between basaltic globules and surrounding magma, the system evolves to the temperature of thermal equilibrium, which is a function of the proportion of basalt to rhyolite, their initial temperatures, and the contribution of the latent heat of crystallization during basalt fractionation.

Table 1 presents temperatures of the final thermal equilibrium at different proportions of basalt to rhyolite, as well as the time needed to reach this equilibrium as a function of the globule size. For the compositions of magmas and initial temperatures assumed in this calculation, the temperature of the final thermal equilibrium can be approximated by a simple polynomial equation

$$T = -209.24\alpha^2 + 674.81\alpha + 1023,$$

where T is the equilibrium temperature in Kelvin and α is the volume fraction of the basalt. The temperature of the final thermal equilibrium increases by 20–65 K as a function of α compared to the calculations excluding the latent heat of crystallization.

Influence of the droplet size and total basalt content on the time required to establish the thermal equilibrium. Time needed to reach thermal equilibrium as a function of the droplet radius and the proportion of basalt in the system, can be described as:

$$t = m\alpha^q R^2,$$

where t is the time in seconds, α is the volume proportion of basalt, R is the radius of basalt drops in meters, and m and q are coefficients.

The results of the calculation of the time needed for establishing the thermal equilibrium between melts for different magma parameters are presented in Table 1. They are approximated well by equation

$$t = 1216534\alpha^{-0.464}R^2. \quad (13)$$

Similarly to the case of the heat conductivity equation with constant coefficients, the time is proportional

to the squared radius of drop R. The coefficient of proportionality decreases with the increasing proportion of basalt because the equilibrium temperature T_{eq} (see the last line in the Table) increases with increasing α, and the degree of cooling of basaltic magma decreases.

Due to an increase in the effective thermal conductivity, the time for establishing thermodynamic equilibrium increases if we take crystallization into account. For the parameters considered here, the cooling time increases by 15–40% depending on the basalt volume fraction.

DISCUSSION OF THE RESULTS AND THE MIXING MECHANISM

The modeling results show that the time of crystallization of basaltic globules is negligibly small compared to the time needed for sufficient diffusive exchange between basaltic and rhyolite melts. Mixing of melts via diffusion and re-equilibration of phenocrysts can not occur during the time between injection of the basaltic melt and eruption (days to months).

At the given proportion of basic to felsic magmas, diffusion plays a greater role at a higher extent of fragmentation and smaller size of the drops. However, as was shown above, the time for cooling and crystallization of drops is proportional to distance squared; therefore, crystallization would always be the main factor over diffusive exchange.

Influence of factors that were not taken into account during modeling and further development of the model. It is assumed in the crystallization model of the basaltic melt drops considered here, that the time of temperature variation at each point of the drop is much greater than the crystallization time of individual crystals. Thus, we neglect the kinetics of crystallization. The rate of crystallization is determined by many parameters, including melt composition, degree of undercooling (the difference between the actual temperature of the melt and its liquidus temperature), presence of nucleation centers, and possibly some other parameters. The melt composition and the degree of undercooling change in the course of crystallization.

In this work, we do not take into account melt–glass transition, which is possible at very high rates of cooling. Glass present in the melanocratic enclaves is a residual melt of rhyolite composition, which agrees well with the model suggested here. However, the possibility cannot be excluded that in other magmatic systems and at greater temperature contrasts, vitrification of the outer zones of basaltic globules is possible immediately after fragmentation, which would lead to significant changes in the mechanism of heat exchange between the globules and surrounding magma. Initially, the melt in a silicic magma chamber can contain phenocrysts and glomeroporphyric aggregations formed from previous intrusions and basalt crystallization. Heating of such magma would lead to partial or complete melting of these crystals, which will make a significant contribution to the thermal balance of rhyolite melt and decrease the temperature, which will be attained after cooling of the droplets. We do not take the dissolution of crystals in the rhyolite into account because there exists many uncertainties of kinetic and thermodynamic nature. We started a systematic study of dissolution kinetics and reactive re-equilibration of crystals with a felsic magma (see, for example, [Plechov et al., 2008] and we plan to take these processes into account during further development of the model.

At present, the model does not take into account the concentration of volatile components in the melt and their influence on the crystallization temperature of minerals. In island-arc magmas rich in volatile components, the influence of water concentration, as well as the difference in solubility of volatile components between basaltic and rhyolite melts, appears to be very strong. As one of the possible scenarios (which is not likely for island arc magmatic systems) it is possible to consider injection of basalt saturated with volatiles into a volatile-poor rhyolite chamber. Due to the low contrast in temperatures, fractionation of basalt could be insignificant, and thermal equilibrium can be established between magmas with contrasting compositions. It is only in this case that chemical mixing becomes possible between rhyolite and basaltic melts. In the article, we discussed a specific example of the Kizimen Volcano, for which independent estimates of temperatures of basaltic and rhyolite magmas were obtained [Trusov and Plechov, 2005]. Both basalt and rhyolite were close to saturation with volatile components at the pressure of the magma chamber (1.2–1.4 kbar), which results in a temperature contrast sufficient to create extensive basalt fractionation.

Degassing of a basaltic melt and nucleation of bubbles will lead to a change in the heat capacity and heat conductivity of the mixture because these parameters in the gas phase differ strongly from those in the melt. The melanocratic enclaves are characterized by abundant bubbles concentrated near the boundaries of enclaves. They merge frequently into one or several large bubbles confined only to one side of the enclaves (it is likely that at the top). Such a distribution of the gas phase allows us to assume that the part of the interface between an enclave and rhyolite insulated by the gas phase was not significant. In addition, the gas phase sorbed at the interface increases the buoyancy of the enclave and possibly causes its motion in the magma chamber, causing the flotation effect suggested for the melanocratic enclaves in magmatic island-arc systems [Bindeman, 1995]. It is likely that flotation explains the effective distribution of basalt globules over the volume of a magmatic chamber.

All the above listed processes require further investigation. However, the suggested mechanism of melt homogenization related to intrusion, fragmentation,

cooling, and crystallization of basalt magma in a rhyolite chamber seems the most probable. Further study of the interaction processes between basaltic and rhyolite magmas requires detailed petrological investigations of magmatic melanocratic enclaves at well-characterized volcanic complexes, aimed at providing data on the thermal history of individual globules and determining the evolution of the globules during their fragmentation, crystallization, and disintegration. Quantitative data gathered on natural samples will allow us to introduce a larger number of parameters into the numerical model as well as to take the kinetics of crystallization and re-equilibration of crystals and melts into account. The development of the model will also include examination of processes of re-equilibration of the silicic magma under increasing temperature.

ACKNOWLEDGMENTS

The authors thank A.A. Barmin, I.N. Bindeman, and L.L. Perchuk for discussions and valuable and constructive remarks. This work was supported by the Russian Foundation for Basic Research (project no. 08-01-00016-a) and the RF President's Program "Russian Leading Scientific Schools" (grant no.5338.2006.5, Perchuk, L.L., the Leader).

REFERENCES

Annen, C. and Sparks, R.S.J., Effects of Repetitive Emplacement of Basaltic Intrusions on Thermal Evolution and Melt

Generation in the Deep Crust, *Earth and Planetary Science Letters*, 2002,vol. 203, pp. 937–955.

Annen, C., Scaillet, B., and Sparks, R.S.J., Thermal Constraints on the Emplacement Rate of a Large Intrusive Complex: the Manaslu Leucogranite, Nepal, Himalaya, *J. of Petrology*, 2006, vol. 47, pp. 71–95.

Ariskin, A. A. and Barmina, G.S., *Modelirovaniye fazovykh ravnovesii pri kristallizatsii bazal'tovykh magm* (Modeling

of Phase Equilibrium during Crystallization of Basalt Magmas), Moscow: MAIK Nauka/Interperiodica, 2000.

Bacon, C.R., Magmatic Inclusions in Silicic and Intermediate Volcanic Rocks, *J. of Geophysical Research*, 1986, vol. 91, pp. 6091–6112.

Bindeman, I.N., A Practical Petrological Method for the Determination of Volume Proportions of Magma Chamber

Refilling, *J. of Volcanology and Geothermal Research*, 1993, vol. 56, pp. 133–144.

Bindeman, I.N., Retrograde Vesiculation of Basalt Magma in Shallow Sources: a Model of Origin of Melanocrate Inclusions in Acid and Intermediate Rocks, *Petrology*, 1995, vol. 3, no. 6, pp. 632–644.

Churikova, T., Worner, G., Eichelberger, J, and Ivanov, B., Minor- and Trace-Element Zoning in Plagioclase from Kizimen Volcano, Kamchatka: Insights on the Magma Chamber Processes, in *Volcanism and Tectonics of the Kamchatka Peninsula and Adjacent Areas, Geophys. Monograph Series*, 2007, vol. 172, pp. 303–324.

Clynne, M. A., A Complex Magma Mixing Origin for Rocks Erupted in 1915, Lassen Peak, California, *J. of Petrology*, 1999, vol. 40, pp. 105–132.

Coombs, M.L. and Gardner, J.E., Reaction Rim Growth on Olivine in Silicic Melts: Implications for Magma Mixing,

Amer. Mineralogist, 2004, vol. 89, 748–759.

Costa, F. and Singer, B.S., Evolution of Holocene Dacite and Compositionally Zoned Magma, Volcan San Pedro, Southern Volcanic Zone, Chile, *J. of Petrology*, 2002, vol. 43, pp. 1571–1593.

Dirksen, O., Humphreys, M.C.S., Pletchov, P., et al., The 2001–2004 Dome-Forming Eruption of Shiveluch Volcano,

Kamchatka: Observation, Petrological Investigation, and Numerical Modeling, *JVGR*, 2006, vol. 155, Is. 3–4, pp. 201–226.

Eichelberger, J.C., Andesitic Volcanism and Crustal Evolution, *Nature,* 1978, vol. 275, pp. 21–27.

Eichelberger, J.C., Izbekov P.E., and Browne, B.L., Bulk Chemical Trends at Arc Volcanoes are not Liquid Lines of

Descent, *Lithos.*, 2006, vol. 87, pp. 135–154.

Feeley, T.C. and Dungan, M.A., Compositional and Dynamic Controls on Mafic-Silicic Magma Interactions at Continental Arc Volcanoes: Evidence from Cordon El Guadal, Tatara-San Pedro Complex, Chile, *J. of Petrology*, 1996, vol. 37, pp. 1547–1577.

Frolova, T.I. and Burikova, I.A., *Magmaticheskiye formatsii sovremennykh geodynamicheskikh obstanovok* (Magmatic

Rock Associations under Modern Geodynamic Conditions), Moscow: Nauka, 1997.

Gorshkov, G.S. and Bogoyavlenskaya, G.E., *Vulkan Bezymyannyi i osobennosti ego poslednego izverzheniya v 1955–1963 gg.* (Besymyannyi Volcano and Peculiarities of Its Last Eruption in 1955-1963), Moscow: Nauka, 1965.

Melekestsev, I.V., Ponomareva, V.V., and Volynets, O.N., Kizimen Volcano (Kamchatka). Is it a future St. Helens? *Vulkanologiya i seismologiya*, 1992, no. 4, pp. 3–32.

Murphy, M.D., Sparks, R.S.J., Barclay, J, et al., Remobilization of Andesite Magma by Intrusion of Mafic Magma at the

Soufriere Hills Volcano, Montserrat, West Indies, *Petrology*, 2000, vol. 41, no. 1, pp. 21–42.

Nakada, S., Motomura, Y., and, Maeda S., Compositional Diversity of Unzen Dome Lavas, *Proceedings, Unzen International Workshop*, Japan, Shimabara, 1997, pp. 78–81.

Naumov, B.V., Kovalenko, V.I., Babansky, A.D., and Tolstykh, M.L., Genesis of Andesites: Evidence from Studies of

Melt Inclusions in Minerals, *Petrologiya*, 1997, vol. 5, no. 6, pp. 586-597; [Petrology, 1997,vol. 5, no. 6, pp. 654–665].

Navon, O., Chekhmir, A., and Lyakhovsky V., Bubble Growth in Highly Viscous Melts: Theory, Experiments, and

Explosivity of Lava Domes, *Earth and Planet. Sci. Letters*, 1998, vol. 160, pp. 763–776.

Pallister, J.S., Hoblitt, R.P., Meeker, G.P., et al., Magma Mixing at Mount Pinatubo: Petrographic and Chemical Evidence from the 1991 Deposits, *Fire and Mud: Eruptions and Lahars of Mount Pinatubo, Philippines*, Univ. of Washington Press, Seattle, 1996, pp. 687–732.

Plechov, P.Yu., Mironov, N.L., Plechova, A.A., and Khubunaya, S.A., Compositional Peculiarities and Genesis of Melt Inclusions in Plagioclase from the Apakhonchich Lava Flow, Klyuchevskoi Volcano, Kamchatka, *Geokhimiya,* 2000, vol. 38, no. 1, pp. 34–42; [Geochemistry International, 2000, no. 1, pp. 39–47].

Plechov, P.Yu., Tsai, A.E., Shcherbakov, V.D., and Dirksen, O.V., Opacitization Conditions of Hornblende in Bezymyannyi Volcano Andesites (March 30, 1956 Eruption), *Petrologiya*, Vol. 16, no. 1, pp. 19–35, 2008 [Petrology, 2008, vol. 16, no. 1, pp. 21–37].

Popov, V.S., Mixing of Magmas is an Important Petrogenetic Process, *Zapiski VMO*, 1983, pp. 229–240.

Trusov, S.V. and Plechov, P.Yu., Formation of Acid-to-Basic Series at Kizimen Volcano (Kamchatka), Mezhdunarodnoe petrograficheskoe coveshchanie *"Petrografiya XXI veka"* (International Petrographic Meeting Petrography in the 21st Century), Apatity, 2005, pp. 48–51.

Wood, B.J., Thermodynamics of Multi-Component Systems with Solid Solutions, in *Thermodynamic Modeling of Geological Materials: Minerals, Fluids, and Melts*, Carmichael, I. and Oygster, H., Eds., London, 1987, pp. 82–110.